Electronic Supplementary Material (ESI) for Nanoscale.

Supporting Information

Boosting Perovskite Nanomorphology and Charge Transport Properties via a Functional D-π-A Organic Layer at the Absorber/Hole Transporter Interface

Mohamed Elsenety[a], Anastasios Stergiou[b], Labrini Sygellou[c], Nikos Tagmatarchis[b], Nikolaos Balis[a], Polycarpos Falaras[a]*

[a]National Centre for Scientific Research "Demokritos", Institute of Nanoscience and Nanotechnology, 15341, Agia Paraskevi Attikis, Athens, Greece

[b]Theoretical and Physical Chemistry Institute, National Hellenic Research Foundation, 48 Vassileos Constantinou Avenue, Athens 11635, Greece

[c]Foundation of Research and Technology Hellas, Institute of Chemical Engineering Sciences, Platani GR-26504, Patras, Greece

AUTHOR INFORMATION

***Corresponding Author**

E-mail address: p.falaras@inn.demokritos.gr; ORCID: 0000-0002-9553-5301

Table S1. Power conversion efficiencies from preliminary tests conducted with D35 introduced into PSCs as an interlayer and during anti-solvent treatment.

Cell structure	**Anti-solvent**		**PCE (%)**
FTO/TiO_2/Perovskite /Spiro-MeOTAD/Ag	Chlorobenzene		15.23
FTO/TiO_2/Perovskite /Spiro-MeOTAD/Ag	D35 in Chlorobenzene	10^{-4} M	16.08
		10^{-5} M	16.56
		10^{-6} M	15.02
FTO/TiO_2/Perovskite/D35 /Spiro-MeOTAD/Ag	Chlorobenzene	10^{-5} M	**18.57**
FTO/TiO_2/Perovskite /FABr/Spiro-MeOTAD/Ag	Chlorobenzene		14.29
FTO/TiO_2/Perovskite/FABr/Spiro-MeOTADAg	D35 in Chlorobenzene	10^{-5} M	16.22
FTO/TiO_2/Perovskite/D35 /FABr/Spiro-MeOTAD/Ag	Chlorobenzene	10^{-5} M	17.17

(a) (b)

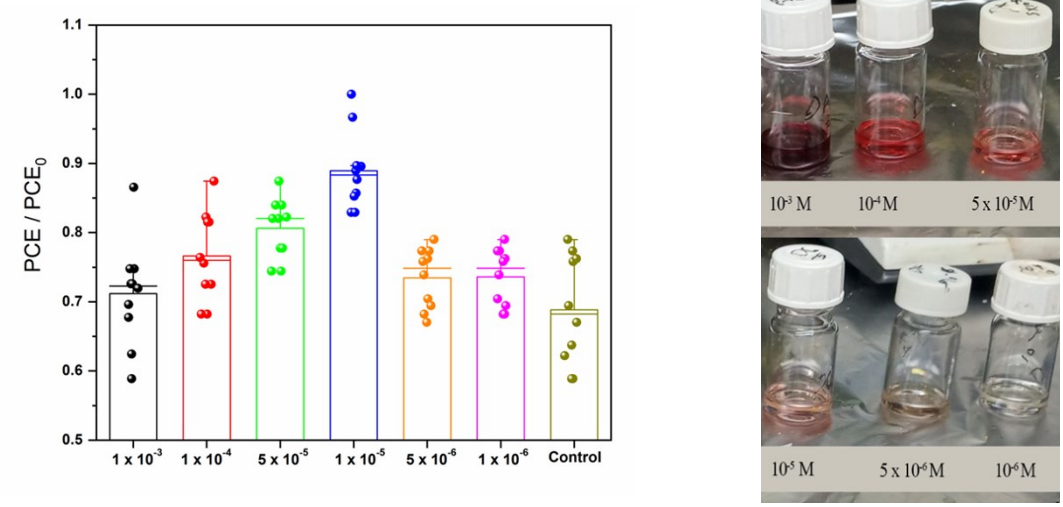

Figure S1. Normalized PCEs of cells, as a function of the D35 concentration (a); Picture of vials with D35 solutions (*10^{-6}M to10^{-3}M)* in chlorobenzene (b).

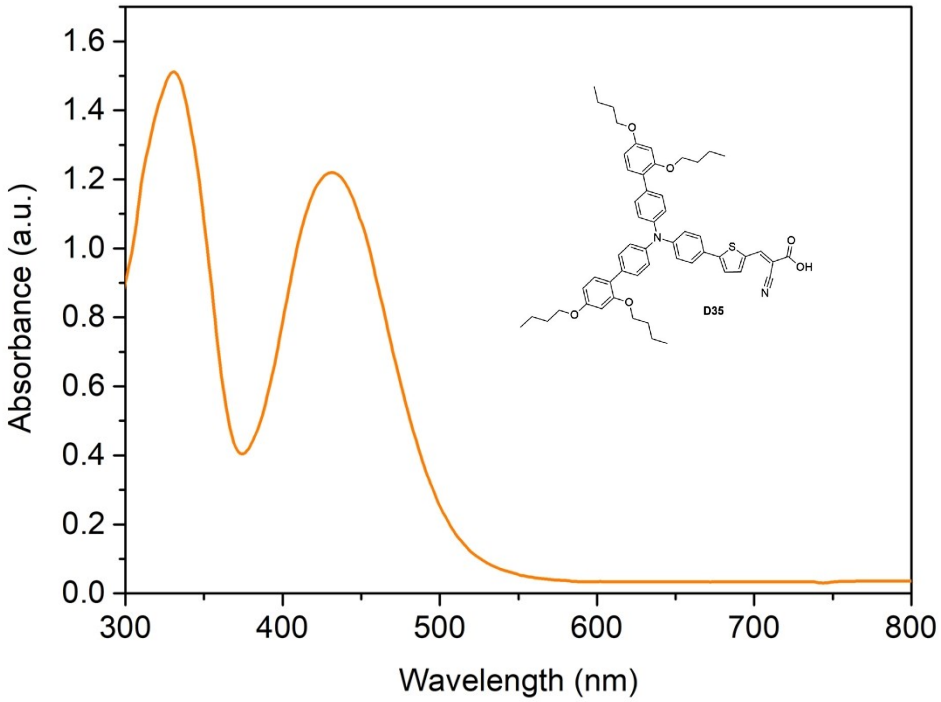

Figure S2. Absorption spectrum of D35 dissolved in chlorobenzene (10^{-5}M); its molecular structure depicting hydrophobic butoxy chains and cyanocrylic acid functional group (inset).

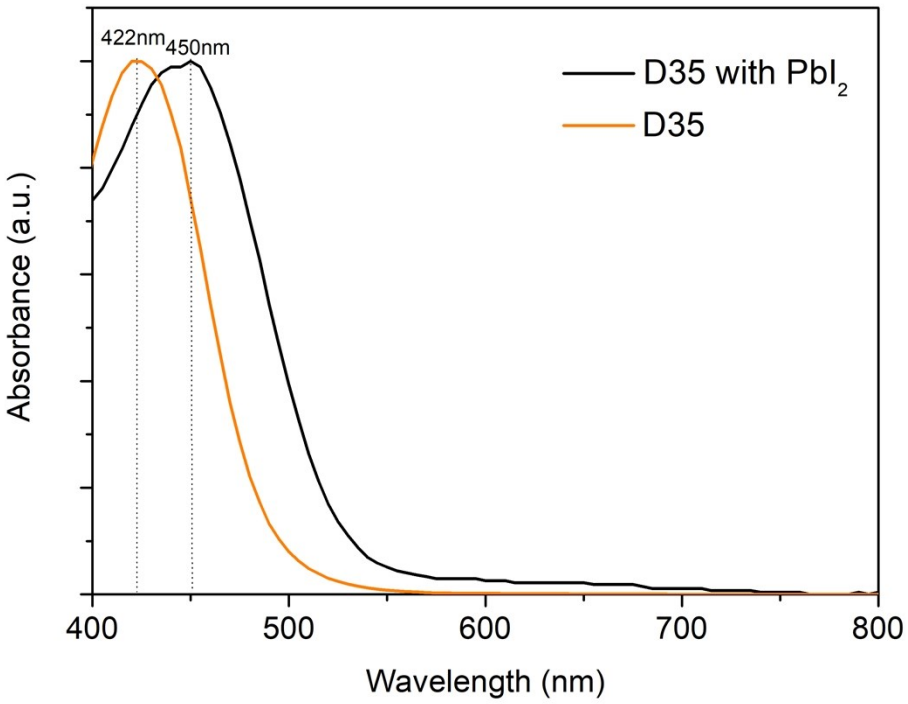

Figure S3. HOMO to LUMO transition shift of D35 solutions with and without PbI_2 (molar ratio 1:1, in chlorobenzene)

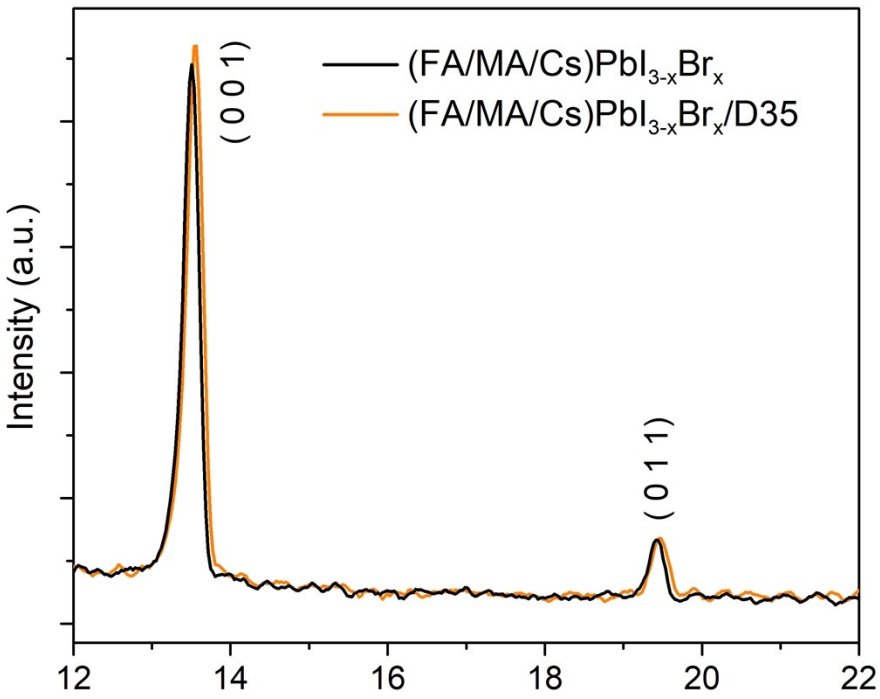

Figure S4. XRD patterns of mixed perovskite films with and without D35 treatment

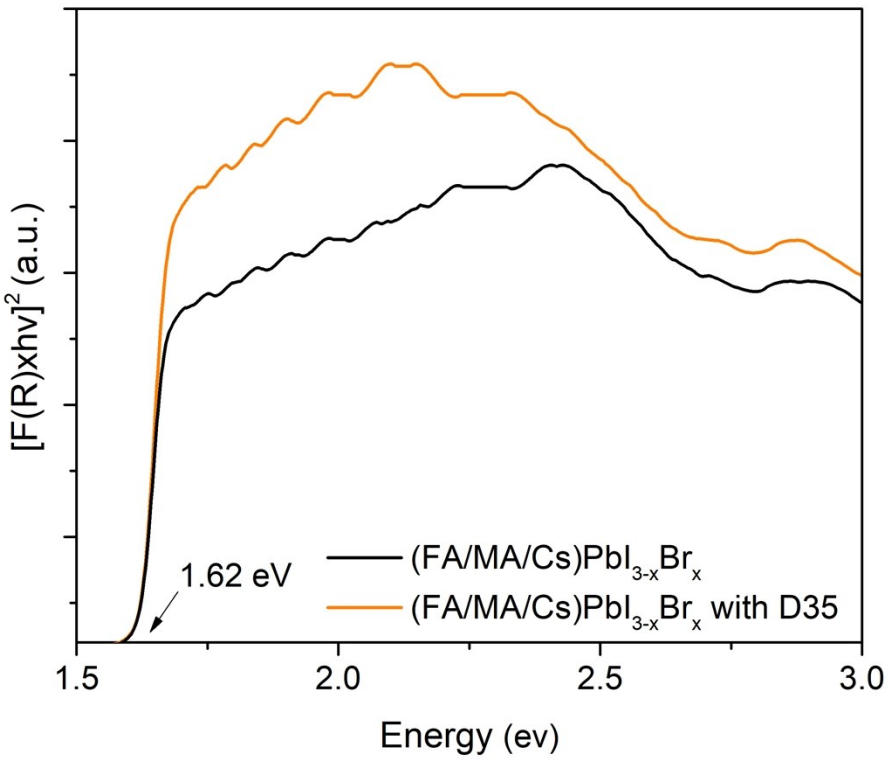

Figure S5. Diffuse reflectance spectra of TiO_2/(FA/MA/Cs)$PbI_{3-x}Br_{x/}$D35 and TiO_2/(FA/MA/Cs)$PbI_{3-x}Br_x$ films.

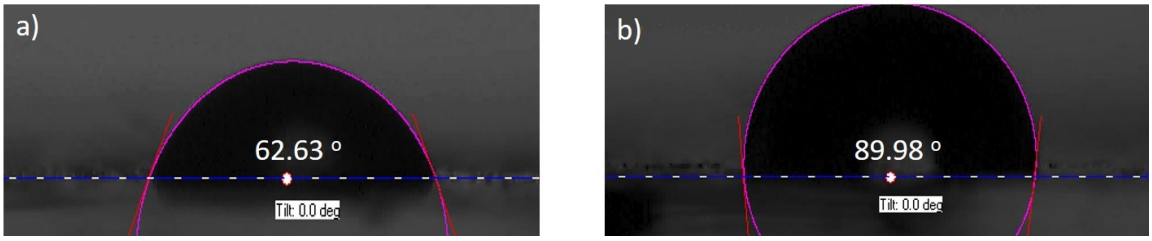

Figure S6. Contact angle measurements of reference and D35- modified films upon mesoscopic TiO_2 surfaces

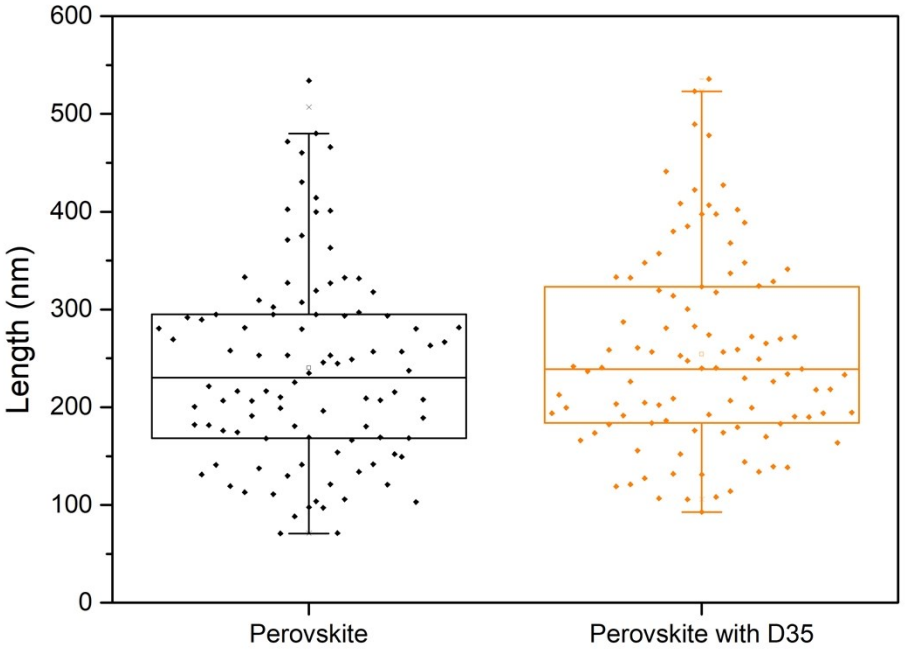

Figure S7. Grain size distribution of (FA/MA/Cs)$PbI_{3-x}Br_x$/D35and (FA/MA/Cs)$PbI_{3-x}Br_x$ films grown on TiO_2 substrates

Table S2. Statistical parameters of the grains size for (FA/MA/Cs)$PbI_{3-x}Br_x$/D35 and (FA/MA/Cs)$PbI_{3-x}Br_x$ films grown on TiO_2 substrates.

Sample	Mean (nm)	Standard deviation (nm)	Minimum(nm)	Median (nm)	Maximum (nm)
Reference	240,44	101,0	70,8	230,2	533,9
D35	254,34	100,0	92,8	239,1	535,7

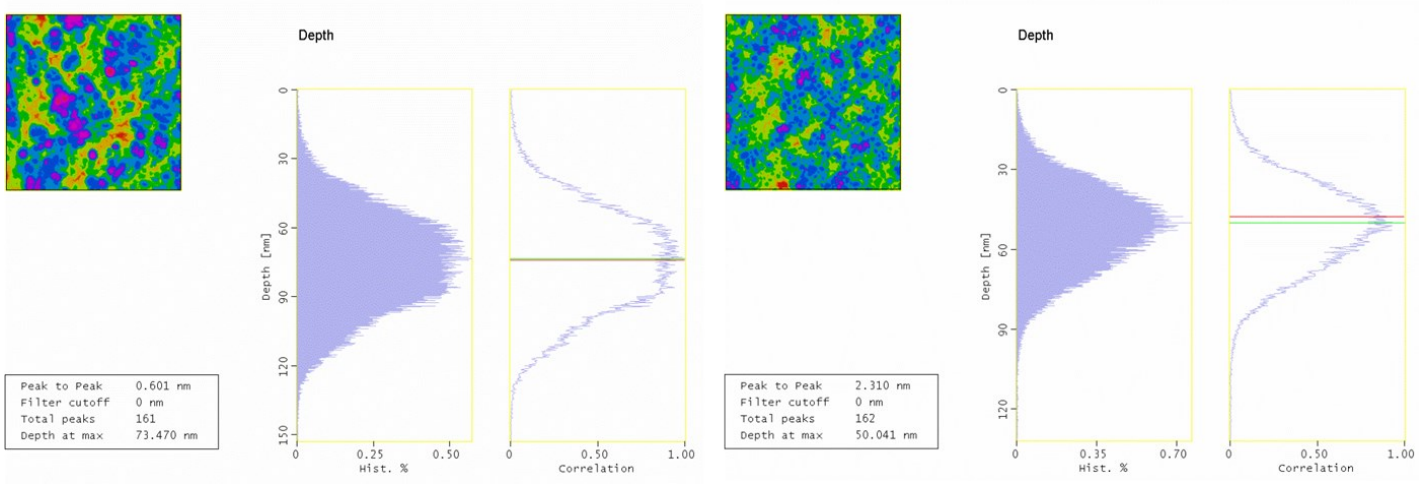

Figure S8. Depth histograms of top surface topography for (FA/MA/Cs)$PbI_{3-x}Br_x$/D35 (right)and (FA/MA/Cs)$PbI_{3-x}Br_x$ (left) films grown on TiO_2 substrates

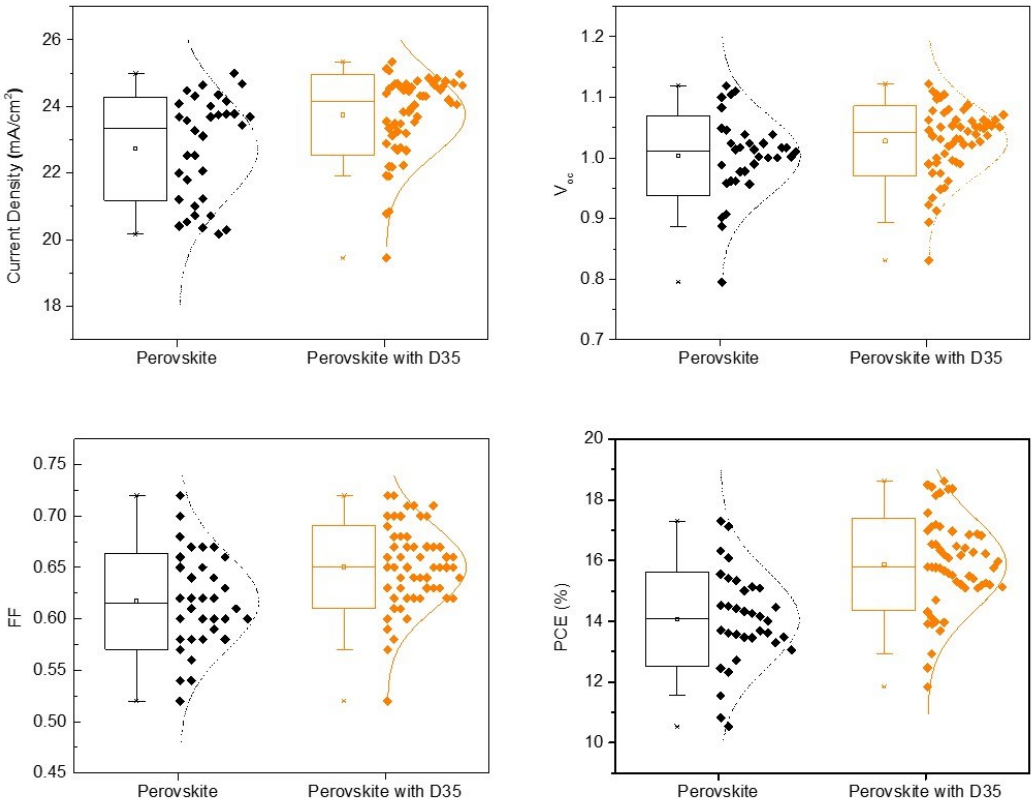

Figure S9. The statistical analysis of the photovoltaic parameters for PSCs with and without D35.

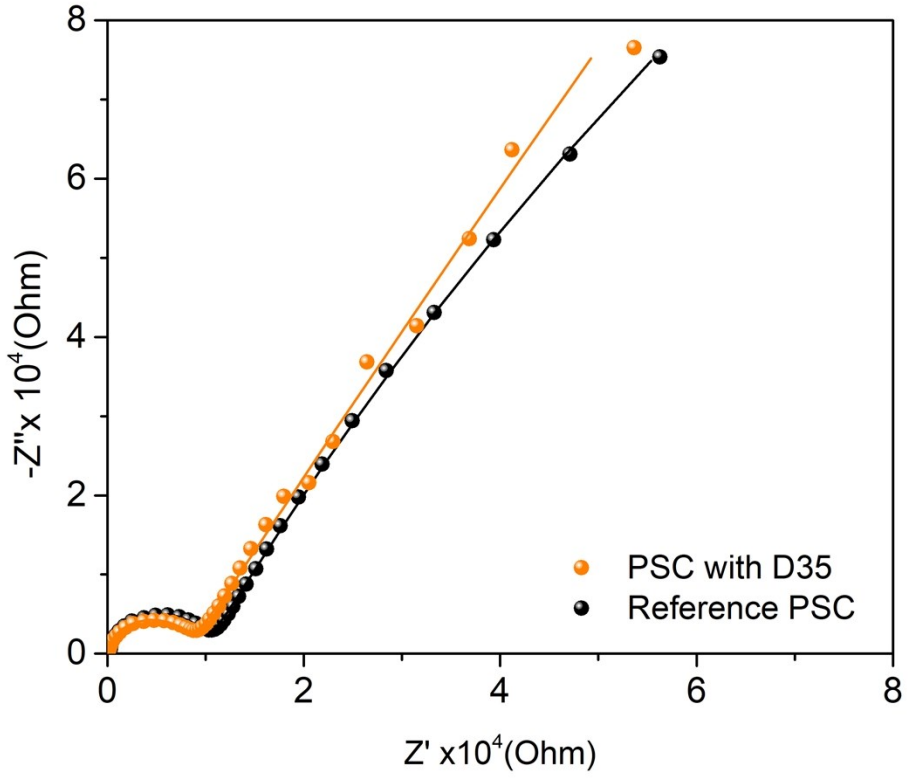

Figure S10. The Nyquist plots obtained via EIS measurements, under dark conditions and under V_{MP} bias. (Fitting of data has been done using the same equivalent electrical circuit as presented in the inset of Figure 7d).

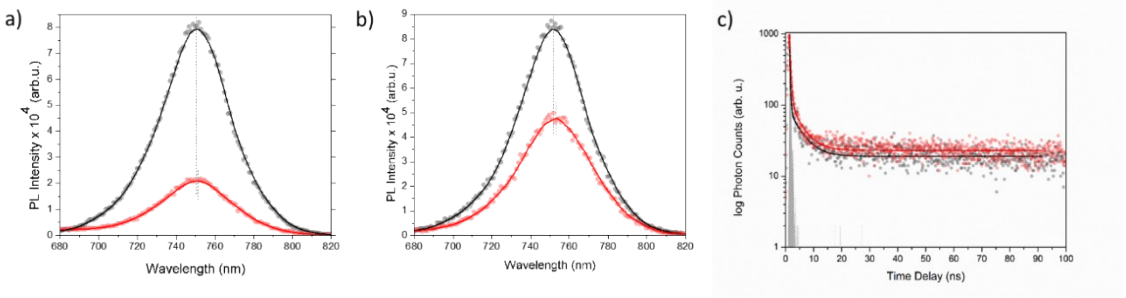

Figure S11. Steady-state photoluminescence spectra of FTO/TiO_2/perovskite (black) and FTO/TiO_2/perovskite/D35 (red) devices at room temperature upon excitation at a) 482 nm, and b) 650 nm. (c) Time-correlated single photon counting spectra obtained under 482 nm excitation and probed at 750 nm at room temperature.

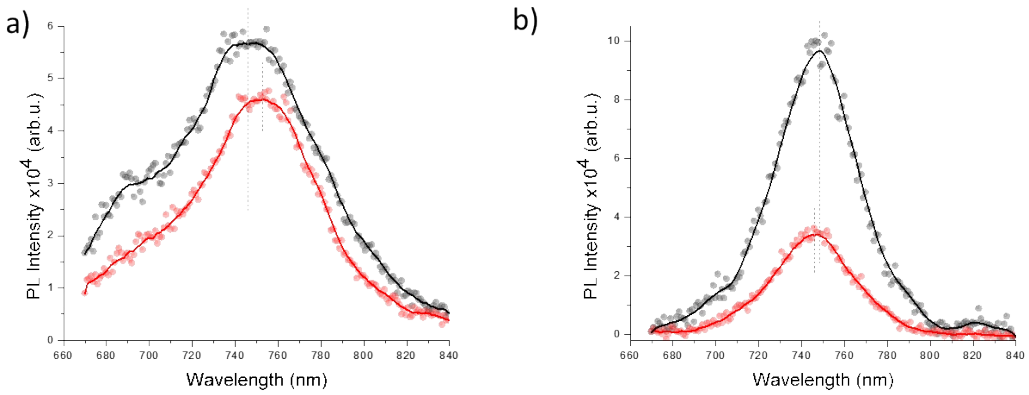

Figure S12. Steady-state photoluminescence spectra of glass/perovskite (black) and glass/perovskite/D35 (red) devices obtained at room temperature upon excitation at 650 nm, irradiated from a) the glass side, and b) the surface side.

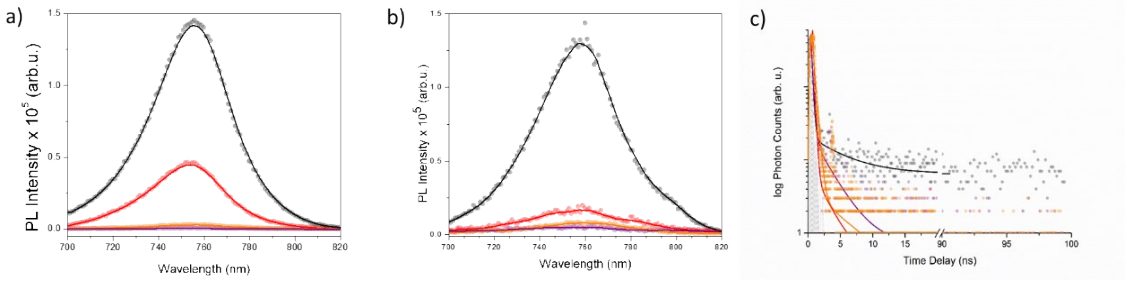

Figure S13. Steady-state photoluminescence spectra of glass/perovskite (black), glass/perovskite/D35 (red), glass/perovskite/Spiro-MeOTAD (purple) and glass/perovskite/D35/Spiro-MeOTAD devices obtained at room temperature upon excitation at a) 482 nm, and b) 650 nm. (c) Time-correlated single photon counting spectra under 482 nm excitation and probed at 750 nm at room temperature.

Table S3. Biexponential fitting of the perovskite's fluorescence emission decay traces recorded via time-correlated single photon counting under 482 nm excitation and probed at 750 nm at room temperature (t: decay lifetime; A: relative population).

Sample	**t_1(ns)**	**A_1**	**t_2(ns)**	**A_2**	**average (ns)**
Glass/perovskite	5.1	0.34	0.209	0.66	1.87
Glass/Perovskite/D35	2.2	0.09	0.201	0.91	0.38
Glass/ Perovskite /Spiro-MeOTAD	2.67	0.21	0.253	0.79	0.76
Glass/ Perovskite /D35/Spiro-MeOTAD	0.25	-	-	-	0.25